Band-structure modifications due to photogenerated carriers in a GaAs/$Al_xGa_{1-x}As$ heterostructure

L. M. Weegels, J. E. M. Haverkort, M. R. Leys, and J. H. Wolter
Department of Physics, Eindhoven University of Technology, P.O. Box 513, NL-5600 MB Eindhoven, The Netherlands
(Received 10 February 1992)

We have investigated, by means of photoluminescence (PL) and photoluminescence excitation (PLE) spectroscopy, the carrier-induced band-structure modifications of a GaAs/$Al_xGa_{1-x}As$ heterostructure containing a two-dimensional electron gas (2DEG). The PL spectra are dominated by an intense recombination line which originates from the 2DEG and which is blueshifted as a function of excitation density. In the PLE spectra, we observe excitonic transitions to unoccupied states of the 2DEG that are also slightly blueshifted. By comparison with self-consistent calculations of the subband structure of the electrons and holes, the origin of the observed transitions can be unambiguously determined. We developed a model in which the carrier-induced band-structure modifications can be calculated, taking into account the contribution of the photogenerated excess carriers. The dominant mechanism which causes the blueshift of the PL spectra is the change of the electrostatic potential due to the buildup of holes, separated in real space from the excess electrons in the 2DEG.

I. INTRODUCTION

In a modulation-doped GaAs/$Al_xGa_{1-x}As$ heterostructure the band structure is partly determined by the separation between the electrons in the two-dimensional electron gas (2DEG) and their parent donors in the $Al_xGa_{1-x}As$ layer. There has been a great deal of interest in studying the 2DEG by means of (magneto)-transport measurements. However, optical investigations of the 2DEG are almost entirely limited to modulation-doped quantum wells (QW's).[1-5] The optical properties of these QW's are well known and are strongly affected when carriers are introduced in the heterostructure. The optical properties of the 2DEG confined at a single heterojunction interface have attracted some attention recently.[6-9]

In this paper we report on the nonlinear optical properties of two-dimensional (2D) electrons at a single GaAs/$Al_xGa_{1-x}As$ interface. We compare experimental data obtained by photoluminescence (PL) and photoluminescence excitation (PLE) spectroscopy with the results of self-consistent band-structure calculations, which include the light-induced modifications due to photogenerated carriers. In this way we are able to disentangle the processes causing the nonlinear optical properties of 2D electrons at a single GaAs/$Al_xGa_{1-x}As$ heterojunction. Moreover, we will demonstrate unambiguously which process dominates these light-induced changes.

Recently, several authors have reported photoluminescence originating from a single GaAs/$Al_xGa_{1-x}As$ heterojunction.[10-12] The luminescence bands shift to higher energies with increasing excitation density. Several recombination mechanisms are proposed: Alferov *et al.*[10] and 't Hooft *et al.*[11] related the luminescence to a defect pair situated at or near the interface of the heterojunction. Yuan *et al.*[12] observed a luminescence band related to the accumulation of photogenerated carriers near the GaAs/$Al_xGa_{1-x}As$ interface. However, these reports dealt with nominally undoped bulk GaAs/$Al_xGa_{1-x}As$ heterojunctions, where no 2DEG is present intrinsically. It appears that the nonlinear optical properties of these heterostructures depend heavily on the design and preparation of the sample. In our studies we use a specially designed modulation-doped heterostructure[13] in which a high-mobility 2DEG is located in a thin GaAs layer of 55-nm thickness. In such a heterostructure a blueshift of a recombination line originating from the 2DEG is observed with increasing excitation density.[7,9] Similar behavior is observed in heterostructures containing a two-dimensional hole gas.[14]

In this paper we report on detailed results obtained by PL and PLE experiments on such a specially designed heterostructure. We observe excitonic transitions due to several excited states of the 2DEG, which we discuss in relation to a model in which the carrier-induced band-structure modifications of the heterostructure are calculated by taking into account the contribution of the photogenerated excess carriers. By comparison with these self-consistent calculations of the band structure the origin of the observed transitions can be unambiguously determined. Thus we can prove that the significant modifications of the band structure arise due to the change of the electrostatic potential as a result of the buildup of photogenerated holes, separated in real space from the excess electrons in the 2DEG.

II. EXPERIMENTAL DETAILS

We studied a modulation-doped heterostructure, grown by molecular beam epitaxy, in which the GaAs layer containing the 2DEG is only 55 nm thick, thus ensuring overlap of the wave functions of the 2DEG and photogenerated holes. The GaAs layer containing the 2DEG is sandwiched between a modulation-doped

$Al_{0.33}Ga_{0.67}As$ layer and a 25 period 5-nm AlAs–5-nm GaAs superlattice. The modulation-doped $Al_{0.33}Ga_{0.67}As$ layer has a thickness of 45 nm, including a 10-nm spacer layer and is n-doped (Si) to 2×10^{18} cm^{-3}. The superlattice is grown on top of a semi-insulating (SI) GaAs substrate. The $Al_{0.33}Ga_{0.67}As$ layer is capped with a 17-nm GaAs layer.

In this study the nonequilibrium carriers are created by the use of a picosecond Styryl-9 dye-laser tunable between 1.35 and 1.56 eV, operating at a repetition frequency of 76 Mhz. The spectral width of the dye-laser pulse is 0.4 meV. In this study we use a maximum excitation density I_0 of 90 W/cm^2. We estimate that at this excitation density 1.3×10^{11} electron-hole pairs per cm^2 per laser pulse are created in the 55-nm-thick GaAs layer containing the 2DEG. For the PL and PLE measurements the average laser intensity is stabilized with a high-bandwidth electro-optic intensity stabilizer. In all experiments the sample is cooled below 2 K in a LHe-bath cryostat.

For transport measurements the sample is processed into a Hall bar with Au-Ge-Ni Ohmic contacts to the 2DEG. A semitransparent 8-nm Au layer is evaporated on top of the Hall bar to serve as a Schottky gate. The electron density is 7.3×10^{11} cm^{-2} and rises to 7.7×10^{11} cm^{-2} under saturated illumination as determined by Hall measurements. The mobility is 3.7×10^5 cm^2/V s.

III. RESULTS OF PL AND PLE

When the sample is excited with light of an energy just above the GaAs band gap, the luminescence at low temperatures originates from the 55-nm-thick GaAs layer and the SI-GaAs substrate. The luminescence of the SI-GaAs substrate is dominated by well-known bulk recombination lines due to donor to acceptor (D, A) and electron to acceptor (e, A) transitions and recombining excitons. In addition to these bulk lines, a new line is observed in the spectrum between the (e, A) transition line at 1.494 eV and the free exciton line at 1.515 eV. By applying a bias to the semitransparent Schottky gate, we have demonstrated[9] that this line originates from electrons of the 2DEG recombining with photogenerated holes. In addition, we have reported that the line is blue-shifted with increasing excitation density. This is also shown in the PL spectra (dashed lines) of Figs. 1 and 2 for three different excitation densities. The recombination line originating from the 2DEG is shifted from 1.504 eV to 1.512 eV, when the light intensity is increased by three orders of magnitude. The PLE spectra with the detection set on the recombination line of the 2DEG are also presented in Figs. 1 and 2 and will be discussed later.

In the PL spectrum of Fig. 1, the recombination line originating from the 2DEG is observed at 1.504 eV (peak 3). For flat-band conditions we expect that the transition energy for electrons in the lowest subband with in-plane wave vectors near zero is approximately equal to $\hbar\omega\approx E_g-E_F$ with E_g the band gap of GaAs and E_F the Fermi energy of the 2DEG. For the sample used in this study ($E_F\approx26$ meV), the transition due to the lowest electron subband e_0 is expected to roughly occur at a photon energy of 1.493 eV. Therefore, we assign the line labeled 3 to a recombination of electrons of the second subband e_1 with holes of the lowest heavy-hole subband: $e_1\rightarrow hh_0$. In addition to transitions of the 2DEG strong luminescence lines originating from the semi-insulating GaAs substrate are detected: donor to acceptor (peak 1), electron to acceptor (peak 2), and exciton transitions

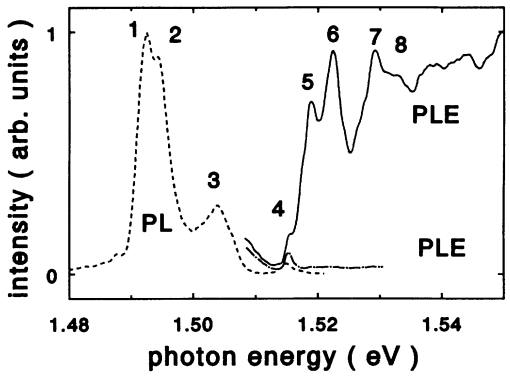

FIG. 1. Photoluminescence spectrum (dashed line) of the modulation-doped heterostructure at an excitation density of 0.045 W/cm^2. The PL spectrum consists of three well-known bulk recombination lines labeled as (1) donor to acceptor (D, A), (2) electron to acceptor (e, A), and (4) excitonic (X) transitions. The line at 1.504 eV, labeled as (3) originates from the second subband of the 2DEG. The photoluminescence excitation spectrum for maximum density of the 2DEG (solid line) shows lines associated with transitions from heavy- and light-hole subbands to unoccupied third and fourth electron subbands: (5) $hh_0\rightarrow e_2$, (6) $lh_0\rightarrow e_2$, (7) $hh_0\rightarrow e_3$, and (8) $lh_0\rightarrow e_3$. The PLE spectrum for minimum electron density (dashed-dotted line) reveals the excitonic peak labeled as (4) from the SI-GaAs substrate. The density of the 2DEG is controlled by applying a bias to the front gate. The detection for both PLE spectra is set on the maximum of the PL line originating from the 2DEG at 1.504 eV.

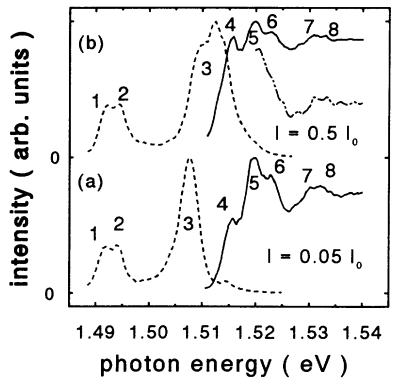

FIG. 2. PL and PLE spectra for two excitation densities (a) $I=0.05I_0$ ($=4.5$ W/cm^2) and (b) $I=0.5I_0$. The PLE spectra are recorded with the detection set at 1.508 and 1.512 eV, respectively. The labeling is the same as in Fig. 1. In the case of $I=0.5I_0$, additional peaks are observed in the PLE spectrum (dashed-dotted line) when the detection is resonant with the $e_2\rightarrow hh_0$ transition at 1.519 eV.

(peak 4). The presence of the substrate luminescence complicates the interpretation of both PL and PLE spectra. However, at low excitation densities the contribution of the substrate can be measured by depleting the 2DEG by applying a bias voltage to the semitransparent Schottky gate. This is shown in the PLE spectra of Fig. 1 for minimum and maximum electron density (respectively, dashed-dotted and solid lines). For recording the PLE spectra, the detection wavelength is tuned to the maximum of the $e_1 \rightarrow \mathrm{hh}_0$ transition. The spectra are taken at an excitation density of $I = 5 \times 10^{-4} I_0 (= 0.045 \mathrm{W/cm}^2)$. The contribution of the substrate to the PLE spectrum is limited to selective pair luminescence[15] below 1.511 eV and the free exciton at 1.515 eV. Above 1.515 eV there is a small constant contribution to the spectrum. Because the $e_1 \rightarrow \mathrm{hh}_0$ transition is observed around 1.51 eV, the $e_0 \rightarrow \mathrm{hh}_0$ transition should occur in the spectral region from 1.47 to 1.49 eV. However, in this spectral region we find that the PL and PLE spectra, not shown in Fig. 1, are dominated by phonon replicas of excitons and of impurity related transitions. These bulk transitions may overshadow the $e_0 \rightarrow \mathrm{hh}_0$ transition.

The PLE spectrum corresponding to the maximum electron density (solid line in Fig. 1) shows resonances corresponding to transitions from hole subbands to higher electron subbands. The doublet at 1.519 and 1.522 eV (peaks 5 and 6) is assigned to transitions from the hh_0 and lh_0 subbands to the third electron subband e_2. The resonance at 1.529 eV (peak 7) and the shoulder at 1.533 eV (peak 8) are due to transitions from the hh_0 and lh_0 subbands to the fourth electron subband e_3.

In Fig. 2 we present representative PL (dashed lines) and PLE (solid lines) spectra for two excitation densities: (a) $I = 0.05 I_0$ and (b) $I = 0.5 I_0$. The detection wavelength is set at the maximum luminescence intensity corresponding to 1.508 and 1.512 eV, respectively. In Fig. 2(a), the lines due to the $\mathrm{hh}_0 \rightarrow e_2$ and $\mathrm{lh}_0 \rightarrow e_2$ transitions now occur at 1.520 and 1.523 eV. Due to broadening effects, the second doublet associated with the fourth electron subband is not resolved. In the case of $I = 0.5 I_0$ [Fig. 2(b)], the detection is set on the low-energy side of the PL line at 1.509 eV to minimize the contribution of the SI-GaAs substrate. When the detection wavelength is near the emission lines of one of the (bound) excitons (1.512–1.515 eV), the PLE spectrum, which is not shown in Fig. 2, is dominated by transitions in the SI-GaAs substrate. In the PLE spectrum of Fig. 2(b), only the doublet at 1.520 and 1.523 eV is well resolved. At these high excitation densities weak luminescence from the third electron subband is detected. When the detection wavelength is near the $e_2 \rightarrow \mathrm{hh}_0$ transition at 1.519 eV, additional resonances are observed in the PLE spectrum (dashed-dotted line) at 1.528 eV, 1.536 eV, and 1.539 eV. These are associated with transitions from higher hole subbands.

IV. THEORY

A. Outline of the calculations

Calculations of the carrier-induced band-structure modifications in a modulation-doped heterostructure should incorporate the photogeneration and subsequent separation of electron-hole pairs occurring in actual spectroscopic experiments. This photogeneration of carriers causes a flattening of the bands in the GaAs layer. Asnin *et al.*[16] have already considered a hole-inversion layer under photoexcitation in *n*-type GaAs. They have calculated the ground-state energy of nonequilibrium electron-hole pairs using Fang-Howard variational wave functions in the Hartree approximation including many-body effects.[17] In their model the nonequilibrium electrons are bound to excess holes in the inversion layer. Their model predicts the experimentally observed blueshift of the luminescence line occurring when the excitation density is increased. However, their model does not account for the complicated band bending in a modulation-doped heterostructure, which cannot be described by Fang-Howard wave functions. Moreover, the calculations are limited to the ground state of electrons and holes.

Since we want to compare the results of the calculations with luminescence spectroscopy, detailed calculations of the subband structure of the heterostructure are necessary. Here, the subband structure for electrons and holes is calculated numerically by solving the Poisson and Schrödinger equation self-consistently within the effective-mass formalism. Photoexcitation of the heterostructure is simulated by taking into account the contribution of the nonequilibrium carriers to the self-consistent potential. We adapt the model of Hurkx and van Haeringen[18] in which the edges of the conduction band, the subband structure, the area density of the 2DEG, and depletion lengths are calculated at zero temperature as a function of material properties and structural parameters. In this model the potential energy for electrons is constructed from the conduction-band discontinuities between the subsequent materials, the electrostatic potential, and the local exchange potential.

Our heterostructure consists of a modulation-doped $\mathrm{Al}_x\mathrm{Ga}_{1-x}\mathrm{As}$ layer adjacent to a thin GaAs layer of thickness L_z, and a semi-infinite $\mathrm{Al}_y\mathrm{Ga}_{1-y}\mathrm{As}$ layer, which simulates the superlattice in the actual sample. Figure 3 gives a real-space sketch of the self-consistent potentials of the heterostructure. There are two depletion regions: $-d_d < z \leq -d_s$ in which both donor and acceptor states are ionized and $-d_s < z \leq d_a$ in which only the acceptor states are ionized. The 2DEG is located in the thin GaAs layer near the $\mathrm{Al}_x\mathrm{Ga}_{1-x}\mathrm{As/GaAs}$ interface at $z = 0$. The electron potential energy $U_e(z)$ can be written as

$$U_e(z) = U_{e_1}\Theta(-z) + U_{e_2}\Theta(z - L_z) + U_c(z) + U_{\mathrm{ex}}(z) , \tag{1}$$

where $\Theta(z)$ is the heaviside unit-step function U_{e_1} between $\mathrm{Al}_x\mathrm{Ga}_{1-x}\mathrm{As}$ and GaAs and U_{e_2} between GaAs and $\mathrm{Al}_y\mathrm{Ga}_{1-y}\mathrm{As}$ at $z = L_z$. The band gap of $\mathrm{Al}_x\mathrm{Ga}_{1-x}\mathrm{As}$ and $\mathrm{Al}_y\mathrm{Ga}_{1-y}\mathrm{As}$ is, respectively, E_{g_1} and E_{g_2}.

The Coulomb potential $U_c(z)$ satisfies the Poisson equation

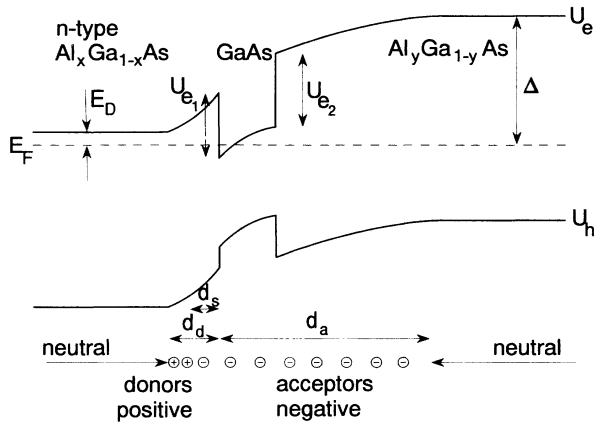

FIG. 3. The schematic energy-band diagram for the heterostructure consisting of a modulation-doped n-type $Al_xGa_{1-x}As$ layer with a spacer layer of thickness d_s, a GaAs layer of thickness L_z, and an $Al_yGa_{1-y}As$ layer. All the layers are slightly and uniformly doped with acceptors. There are two depletion regions: $-d_d < z \leq -d_s$ with completely ionized donors and acceptors and $-d_s < z \leq d_a$ in which only the acceptors are ionized. The building up of a 2DEG will occur in the GaAs layer near the $Al_xGa_{1-x}As/GaAs$ interface. For $z \rightarrow -\infty$ the Fermi level E_F coincides with the donor level, positioned an energy E_D below the conduction band. For $z \rightarrow \infty$ the conduction band is located an energy Δ above the Fermi level.

$$\frac{d^2U_c}{dz^2} = \frac{e\rho(z)}{\epsilon_0\epsilon_r} , \tag{2}$$

where $-e$ is the electron charge, ϵ_0 the permittivity of free space, and ϵ_r the relative dielectric permittivity of GaAs. The charge-density function $\rho(z)$ is the sum of the space-charge density of ionized donors and acceptors, the electron-density function $n(z)$, and the hole-density function $p(z)$, which represents the distribution of photogenerated holes in the PL experiments.

For the exchange and correlation potential $U_{ex}(z)$, we use a local-density approximation[19]

$$U_{ex}(z) = -0.0783\frac{e^2}{\epsilon_0\epsilon_r}[n(z)]^{1/3} . \tag{3}$$

From the potential for electrons, we construct the potential for holes by assuming that the minimum of the valence band is coupled to the minimum of the conduction band with an energy equal to the renormalized band gap of each material. For the holes, the inclusion of the exchange and correlation effects is more difficult because of the complicated subband structure of the valence bands. Here, we approximate the contribution to the hole potential simply by exchanging the electron density in (3) by the hole density. In addition, mixing between the valence subbands of light (lh) and heavy (hh) holes is not considered because of the relatively large width of the GaAs layer containing the 2DEG. A more accurate method is to calculate the subband structure within the random-phase approximation using the actual confinement potential and screened Coulomb potential.[20] However, we estimate the level of inaccuracy as a result of our approximations to be of the order of 1 or 2 meV because of the low photogenerated hole densities used in our samples (less than 10^{11} cm^{-2}). This small inaccuracy still allows a meaningful comparison with experimental results.

The equations to be solved self-consistently are the one-dimensional Schrödinger equation of electron (e) and hole (h) envelope functions, respectively, χ_i^e and χ_j^h,

$$\left[-\frac{\hbar^2}{2m_e^*}\frac{d^2}{dz^2} + U_e(z) - E_i^e\right]\chi_i^e = 0 \tag{4}$$

and

$$\left[-\frac{\hbar^2}{2m_h^*}\frac{d^2}{dz^2} + U_h(z) - E_j^h\right]\chi_j^h = 0 , \tag{5}$$

where m_e^* and m_h^* are the effective masses of the electrons and holes. The effective masses are not varied through the interfaces and are independent of the energy.

In the PL experiments the heterostructure is illuminated with light with a photon energy below the band gap of n-type $Al_xGa_{1-x}As$. Hence, no excess carriers are generated in the n-type $Al_xGa_{1-x}As$ layer and the Fermi level is not affected. For $z \rightarrow -\infty$ and at zero temperature the potential energy $U_e(z)$ coincides with the donor level with an energy E_D below the conduction band in the n-type $Al_xGa_{1-x}As$ bulk material. If we define the energy to be zero at the Fermi level E_F, it follows that

$$U_e(-\infty) = E_D \tag{6}$$

as a boundary condition for the electron potential.

Before illumination the Fermi level in the semi-infinite $Al_yGa_{1-y}As$ layer is identified with the acceptor energy level in the lightly p-type $Al_yGa_{1-y}As$ bulk material. A large depletion layer from the $Al_xGa_{1-x}As/GaAs$ heterojunction at $z=0$ into the $Al_yGa_{1-y}As$ layer is formed. In this layer all acceptors are negatively charged. Thus $U_e(\infty) = E_{g_2} - E_A$, where E_{g_2} is the band-gap energy of $Al_yGa_{1-y}As$ and E_A is the acceptor level above the valence band. After or during illumination, the width of this depletion layer is changed due to the neutralization of ionized acceptors by photogenerated holes. The decrease of the negative charge of this depletion layer is compensated for by increasing the density of the 2DEG. It is reasonable to assume that the radiative recombination time of the electrons of the 2DEG and photogenerated holes in the thin GaAs layer is much shorter than the tunneling time of electrons of the 2DEG to distant neutral acceptors in the $Al_yGa_{1-y}As$ layer. We thus assume that the band bending in the $Al_yGa_{1-y}As$ layer is fixed on the time scale involved in radiative recombination processes. The change of the width and the total charge of the negatively charged depletion layer is taken into account by adjusting the offset of the conduction band for $z \rightarrow \infty$, as follows:

$$U_e(\infty) = \Delta \leq E_{g_2} - E_A . \tag{7}$$

The overlap of the hole and electron envelope functions as well as the transition energies are determined by the boundary condition (7), because the total depletion charge in the $Al_yGa_{1-y}As$ layer determines the electric field in the thin GaAs layer.

In actual samples the total charge in the depletion region and the position of the Fermi level in the epitaxial layers on top of the SI-GaAs substrate are unknown. By changing the parameter Δ we can approximate the position of the Fermi level in the SI-GaAs substrate and epitaxial layers of the actual sample. The parameter Δ is assumed to be constant as a function of the laser intensity.

The calculations are carried out in two iteration procedures. In the first iteration procedure the potential $U_e(z)$ is calculated with (6) and (7) as boundary conditions. The contribution of the photogenerated holes in the thin GaAs layer is not taken into account by putting $p(z)=0$. The band-bending offset parameter Δ is adjusted to give the best fit to the experimental transition energies. The calculated transition energies are determined in the second iteration procedure. Thus, in the first procedure the static response of the band structure is calculated self-consistently.

In the second iteration procedure the depletion length d_a and the band-bending offset parameter Δ are constant. A positive charge distribution of holes is included in the charge distribution function $\rho(z)$ as a result of the generation of electron-hole pairs in the thin GaAs layer. The holes, with an area density of $N_{e\text{-}h}$, are confined in the lowest hole eigenstate. A region of neutral acceptors in the thin GaAs layer is formed if $p(z)>N_A$. To compensate for the change in the number of ionized acceptors and holes $N_{e\text{-}h}$, the density of the 2DEG is increased. The excess electrons of the 2DEG, the holes as well as the region of neutral acceptors in the GaAs layer, contribute to the potential energies of the holes and electrons via the Poisson equation. The second iteration procedure is stopped when the potentials $U_e(z)$ and $U_h(z)$ are calculated self-consistently.

In this way, the transition energies are calculated as a function of the excess density $N_{e\text{-}h}$, material and structural parameters and the band-bending offset parameter Δ. The band-bending offset parameter is the only adjustable parameter in our calculations and is fitted to the experimental data.

B. Results

In Fig. 4 the potentials $U_e(z)$ and $U_h(z)$, the squared envelope functions for the first and second electron subband (respectively, e_0 and e_1), and the first heavy-hole subband (hh_0) are shown both in the dark and illuminated. The donor and acceptor concentrations are 1.5×10^{18} cm^{-3} and 2×10^{14} cm^{-3}, respectively. Furthermore, $L_z=55$ nm, $E_D=50$ meV, $E_A=26$ meV, $E_g=1.519$ eV, $E_{g_2}=2.1$ eV, $U_{e_1}=0.273$ eV, $U_{e_2}=0.389$ eV, $m_e^*=0.067m_0$, $m_{hh}^*=0.45m_0$, $m_{lh}^*=0.10m_0$, and $\epsilon_r=13$. The offset ratio between the conduction-band and valence-band discontinuities is taken to be 67:33. The depletion lengths are found to be $d_d=15.4$ nm in the n-type $Al_xGa_{1-x}As$ layer and $d_a=2.16$ μm in the $Al_yGa_{1-y}As$ layer with the constant band-bending offset parameter Δ set on 1.05 eV. This value of the offset parameter gives the best fit to the experimentally observed transitions, which are described in Sec. III. In the dark, the calculated area density of the 2DEG is 7.63×10^{11} cm^{-2} of which 2.3% is occupied by the second subband. The spacing between the lowest unoccupied electron subbands, e_2 and e_3, is approximately 11 meV, between the light-hole subbands lh_0 and lh_1 9 meV, and the heavy-hole subbands hh_0 and hh_1, 5 meV. According to the cal-

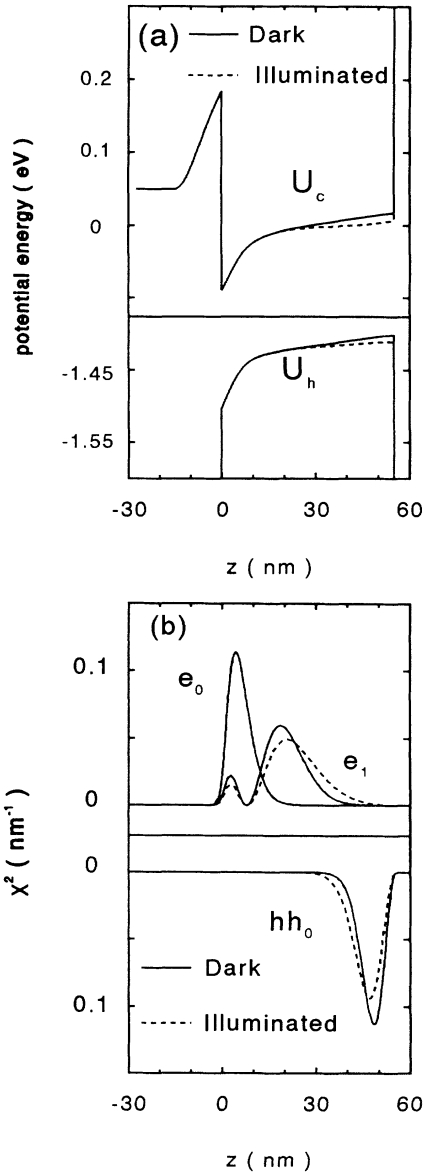

FIG. 4. (a) The conduction- and valence-band edges are shown vs depth in the dark (solid line) and illuminated (dashed line). (b) Normalized envelope functions χ_0^e and χ_1^e of the first and second electron subband and χ_0^{hh} of the first heavy-hole subband in the dark (solid lines) and illuminated (dashed lines). In the illuminated case the density of photogenerated holes is 4×10^{10} cm^{-2}.

culations the holes are therefore quantized at low temperatures. Note that the electron and hole states are separated in real space. Consequently the probability for optical transitions is proportional to the square of the overlap integral S between the hole and electron envelope functions. The ratio of the probabilities of transitions between the two occupied electron subbands and the first heavy-hole subband, $e_1 \rightarrow \mathrm{hh}_0$ and $e_0 \rightarrow \mathrm{hh}_0$, is calculated to be more than 6×10^3 and is weakly dependent on $N_{e\text{-}h}$. Hence, the intensity of the $e_0 \rightarrow \mathrm{hh}_0$ transition should be very weak compared with the intensity of the $e_1 \rightarrow \mathrm{hh}_0$ transition. The transitions associated with the occupied electron subbands show a blueshift in the order of 5 meV. The shift of transitions associated with unoccupied electron subbands is in the order of 1 meV. In Fig. 5 the experimentally observed and the calculated transitions are shown as a function of the excitation density.

V. DISCUSSION

As Fig. 5 demonstrates, the overall agreement between calculations and experiments is good. The trends observed in the experiments can be explained by the theoretical model. Now we comment on the modifications of the band structure induced by the nonequilibrium electron-hole pairs. During illumination, electron-hole pairs are created and subsequently separated by the depletion field in the GaAs layer. The electrons contribute to the 2DEG and the holes pile up near the AlAs barrier or they are captured by ionized acceptors in the GaAs layer. One or a combination of these three mechanisms may cause changes to the band structure, i.e., (1) the increase of the electron density of the 2DEG, (2) neutralization of the negatively ionized acceptors in the thin GaAs layer by photocreated holes, and (3) separation of photocreated electron-hole pairs in the GaAs layer due to the built-in electric field.

As mentioned in Sec. II, the density of the 2DEG is increased only 5% under saturated illumination. This results in a rise of the Fermi level of about 1.5 meV, which is too small to account for the blueshift. This rules out possibility (1).

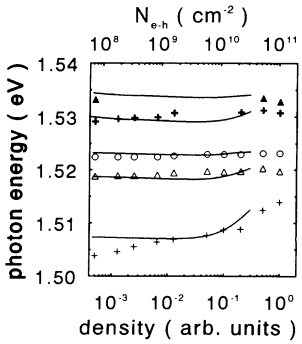

FIG. 5. The experimentally observed transitions (markers) are shown vs the excitation intensity normalized to $I_0=90$ W/cm^2. In the PL spectra: +, $e_1 \rightarrow \mathrm{hh}_0$. In the PLE spectra: △, $\mathrm{hh}_0 \rightarrow e_2$; ○, $\mathrm{lh}_0 \rightarrow e_2$; +, $\mathrm{hh}_0 \rightarrow e_3$; ▲, $\mathrm{lh}_0 \rightarrow e_3$. The solid lines are calculated transition energies where I_0 corresponds to $N_{e\text{-}h}=1.3\times10^{11}$ cm^{-2}.

The second possible mechanism, i.e., neutralization of acceptors in the thin GaAs layer, gives rise to a reduction of the depletion field and a flattening of the conduction and valence bands near the $Al_yGa_{1-y}As$ barrier. This process results in an extra potential difference due to the photoneutralization near the barrier equal to

$$-\frac{e^2N_Ad_n^2}{2\epsilon_0\epsilon_r}, \tag{8}$$

where d_n is the width of the neutralized acceptor region. In the case of $N_A\approx2\times10^{14}$ cm^{-3} and $d_n\approx20$ nm, we calculate that the reduction is very small: 0.056 meV. Thus in our lightly doped GaAs layers, the photoneutralization of acceptors is too small to account for the blueshift in the PL spectra.

When the sample is illuminated, the electrons quickly drift to the 2DEG and a buildup of holes occurs in the 55-nm GaAs layer near the superlattice barrier. In our calculations, the contribution of this positive charge distribution of holes is added to the electrostatic potential energy via the Poisson equation. The formation of such a positive charge distribution separated from the excess electrons in the 2DEG results in a negative shift of the band minima in the region near the $Al_yGa_{1-y}As$ barrier with respect to the Fermi level of the 2DEG, as is shown in Fig. 4(a). As a result, the band bending near the $Al_yGa_{1-y}As$ barrier is reduced and the position of the energy levels is changed in such a way that the transition energies increase. This effect is analogous to charging a parallel-plate capacitor. The potential difference between the charged plates is proportional to the charge Q and distance d according to

$$\Delta V=\frac{Qd}{\epsilon_0\epsilon_r}. \tag{9}$$

In our case, one plate is formed by the excess electrons of the 2DEG and the second one by the holes piled up near the $Al_yGa_{1-y}As$ barrier. If we put d equal to the difference of the average distance of the holes and the electrons in the second subband and $Q=eN_{e\text{-}h}$, we find $\Delta V=13$ meV in the case of $N_{e\text{-}h}=4\times10^{10}$ cm^{-2} and $d=23$ nm. This potential difference is indeed comparable to the shift of 11.7 meV of the potential in Fig. 4(a). Therefore we conclude that the spatial separation of the excess carriers is the dominant mechanism to cause the band-structure modifications. The spatial separation results in a potential difference between the two carrier sheets and a modification of the potentials for electrons and holes in such a way that the transition energies increase.

As shown in Fig. 5, the calculated energy of the $e_1 \rightarrow \mathrm{hh}_0$ transition deviates from the experimentally observed one in the low and high excitation regime. At low excitation densities, the attraction between the excess electrons in the 2DEG and the holes results in a binding of the holes to the 2DEG, which is not included in our calculations. As reported earlier,[9] the thermal ionization energy is estimated to be 1.5 meV. This is in agreement

with the calculated binding energy of 1 meV by Balslev,[21] who considered the formation of excitonic states with the 2DEG. At low excitation densities ($I < 1$ W/cm^2 or $N_{e\text{-}h} < 1.4\times10^9$ cm^{-2}) this extra binding energy can explain the difference between calculated and experimental energy of the transition $e_1 \rightarrow hh_0$, observed in the PL spectra.

At moderate excitation densities, the binding energy is expected to vanish due to phase-space filling.[22] At these densities the calculations appear to be in good agreement with experiments.

The difference between the measured and calculated transition energies in the high excitation regime ($I > 10$ W/cm or $N_{e\text{-}h} > 1\times10^{10}$ cm^2) can be explained by carrier heating after excitation with an intense optical pulse. After excitation the effective-carrier temperature is higher than the lattice temperature. With increasing time delay after the excitation pulse the carrier temperature and density decrease due to cooling and recombination processes. Especially, when the cooling time is comparable to the radiative-decay time, hot carriers contribute to the emission spectrum. The weak luminescence of the third electron subband in the case of $I = 0.5I_0$ [Fig. 2(b)] is due to thermal occupation. If we assume an effective carrier temperature of 50 K ($kT \approx 4$ meV), the holes are distributed over several subbands and give rise to extra peaks which result in a broad luminescence spectrum at 1.514 eV ($I = 0.5I_0$: $e_1 \rightarrow lh_0$) and at 1.515 eV ($e_1 \rightarrow lh_1$).

VI. CONCLUSION

We have compared self-consistent calculations with the results of luminescence spectroscopy on a 2DEG in a GaAs/$Al_xGa_{1-x}As$ heterostructure. We developed a model in which the contribution of the excess photogenerated carriers to the self-consistently determined potential is taken into account. With this model the origin of the transitions observed in PL and PLE spectra can unambiguously be determined. Moreover, the blueshift of the recombination line of electrons of the 2DEG and photogenerated holes can be ascribed to light-induced band-structure modifications. The dominant contribution to these modifications is due to the change of the electrostatic potential as a result of the buildup of holes which are spatially separated from the excess electrons in the 2DEG. We find good agreement between our model calculations and the experimental results.

[1] A. Pinczuk, J. Shah, R. C. Miller, A. C. Gossard, and W. Wiegmann, Solid State Commun. **50**, 735 (1984).

[2] R. C. Miller and D. A. Kleinman, J. Lumin. **30**, 520 (1985).

[3] C. Delalande, Phys. Scr. **T19**, 129 (1987).

[4] H. Yoshimura, G. E. W. Bauer, and H. Sakaki, Phys. Rev. B **38**, 10 791 (1988).

[5] A. S. Chaves, A. F. S. Penna, J. M. Worlock, G. Weimann, and W. Schlapp, Surf. Sci. **170**, 618 (1986).

[6] I. V. Kukushkin, K. v. Klitzing, and K. Ploog, Phys. Rev. B **37**, 8509 (1988).

[7] Q. X. Zhao, J. P. Bergman, P. O. Holtz, B. Monemar, C. Hallin, M. Sundaram, J. L. Merz, and A. C. Gossard, Semicond. Sci. Technol. **5**, 884 (1990).

[8] Q. X. Zhao, Y. Fu, P. O. Holtz, B. Monemar, J. P. Bergman, K. A. Chao, M. Sundaram, J. L. Merz, and A. C. Gossard, Phys. Rev. B **43**, 5035 (1991).

[9] L. M. Weegels, J. E. M. Haverkort, M. R. Leys, and J. H. Wolter, Superlatt. Microstruct. **10**, 143 (1991).

[10] Zh. I. Alferov, A. M. Vasil'ev, P. S. Kop'ev, V. P. Kochereskho, I. N. Ural'tsev, Al. L. Efros, and D. R. Yakovlev, Pis'ma Zh. Eksp. Teor. Fiz. **45**, 442 (1986) [JETP Lett. **43**, 569 (1986)].

[11] G. W. 't Hooft, W. A. J. A. van der Poel, L. W. Molenkamp, and C. T. Foxon, Appl. Phys. Lett. **50**, 1388 (1987).

[12] Y. R. Yuan, M. A. A. Pudensi, G. A. Vawter, and J. L. Merz, J. Appl. Phys. **58**, 397 (1985).

[13] K. Ploog and A. Fisher, Appl. Phys. Lett. **48**, 1392 (1986).

[14] W. Ossau, T. L. Kuhn, E. Bangert, and G. Weimann, in *High Magnetic Fields in Semiconductor Physics II*, edited by G. Landwehr, Springer Series in Solid-State Sciences Vol. 87, (Springer, Berlin, 1989), p. 268.

[15] H. Tews, H. Venghaus, and P. J. Dean, Phys. Rev. B **19**, 5178 (1979).

[16] V. M. Asnin, A. A. Rogachev, A. Yu. Silov, and V. I. Stepanov, Solid State Commun. **74**, 405 (1990).

[17] V. M. Asnin, A. A. Rogachev, V. I. Stepanov, and A. B. Churilov, Pis'ma Zh. Eksp. Teor. Fiz. **45**, 436 (1987) [JETP Lett. **45**, 558 (1987)].

[18] G. A. M. Hurkx and W. van Haeringen, J. Phys. C **18**, 5617 (1985).

[19] W. Kohn and L. J. Sham, Phys. Rev. **140**, A1133 (1965).

[20] G. E. W. Bauer and T. Ando, J. Phys. C **19**, 1537 (1986).

[21] I. Balslev, Semicond. Sci. Technol. **2**, 437 (1987).

[22] D. A. Kleinman, Phys. Rev. B **32**, 3766 (1985).